Front. Earth Sci. 2013, 7(3): 384–394
DOI 10.1007/s11707-013-0382-y

RESEARCH ARTICLE

Flooding impact on the distribution of microbial tetraether lipids in paddy rice soil in China

Asma AYARI, Huan YANG, Shucheng XIE (✉)

State Key Laboratory of Biogeology and Environmental Geology, China University of Geosciences, Wuhan 430074, China

Abstract Isoprenoid and branched glycerol dialkyl glycerol tetraethers (GDGTs) lipids were studied in flooded and non-flooded paddy soil in Wuhan, central China, to examine the response of the GDGTs distribution to the soil flooding. Samples were collected before and after the soil flooding in four specific months. Both core (CL) and intact polar (IPL) GDGTs were quantified. Increase in the abundance of archaeol and caldarchaeol may be indicative of the occurrence of methanogens in the flooded soil. A negative correlation was observed between the ratio of IPL branched GDGT-IIa to GDGT-Ia and the soil pH. The rise of the soil pH in the acid soil is known to be controlled by the redox conditions resulting from flooding. Thus, the branched GDGTs distribution may be controlled by the water content in the paddy soil. In addition, we suggest that the anoxic conditions resulting from flooding may also control the abundance of branched GDGTs relative to crenarchaeol, which in turn results in the increase of branched and isoprenoidal tetraethers (BIT) values, the index for the terrestrial input to the marine sediments.

Keywords glycerol dialkyl glycerol tetraethers (GDGTs), soil flooding, soil pH, redox conditions, GDGTs distribution, branched and isoprenoidal tetraethers (BIT)

1 Introduction

The branched glycerol dialkyl glycerol tetraethers (bGDGTs) are membrane lipids of as-yet unknown bacteria, which have been detected in a wide range of terrestrial environmental settings (Weijers et al., 2006,2007b; Huguet et al., 2010a,2012; Yang et al., 2011,2012). The relative abundance of the methyl moieties, expressed as Methylation of Branched Tetraethers (MBT) index, has been found to relate to the mean annual air temperature (MAT) and the soil pH, whereas the Cyclisation of Branched Tetraethers (CBT) index, showing the relative abundance of cyclopentyl moieties, is related to the soil pH (Weijers et al., 2007b). The linear correlation between MBT, CBT, and MAT therefore provides a new paleothermometer, and has been applied to estimate the temperature variation in estuary sediments and loess-paleosol of different geological ages (Weijers et al., 2007a; Peterse et al., 2011). However, the global calibrations of MBT/CBT with MAT by either Weijers et al. (2007b) or Peterse et al. (2012) both have large scatters, implying that these proxies may be also influenced by other environmental factors in addition to temperature and pH. In fact, it seems that the bGDGTs distribution may be affected by the abundance of water in soil (Loomis et al., 2011) and peat (Huguet et al., 2010a). In addition, the branched and isoprenoidal tetraethers (BIT) index (Hopmans et al., 2004) has been developed to trace soil organic matter in marine environment. This index is based on the observation that the bGDGTs were predominantly produced in terrestrial environments, and the crenarchaeol is mainly derived from marine thaumarchaeota. The BIT value of 1 represents the soil end member and a value of 0 the marine end member. This index has been applied in lacustrine environments (Tierney and Russell, 2009), but recent work on modern soils reveals caution should be taken in applying this index (Yang et al., 2012).

However, little work has been done concerning the environmental impact on GDGTs distribution in paddy rice soils. The irrigated paddy field is a typical wetland habitat in terrestrial ecosystems, which has served as a useful model for biogeochemistry and microbiological studies. Because rice roots release oxygen, the paddy soil forms a unique environment: the rhizosphere is partially oxic, while the bulk soil is anoxic (Revsbech et al., 1999). In addition, rice paddy soil is one of the dominant sites of methane release, suggesting the occurrence of an abundant diversity of methanogenic archaea on rice roots (Lu et al., 2005), in rhizosphere (Lu and Conrad, 2005), and in the

Received January 24, 2013; accepted April 11, 2013

E-mail: xiecug@163.com

bulk soil (Großkopf et al., 1998). The change in the degree of the soil moisture of the paddy rice fields provides an opportunity to study the environmental control on the distribution of the GDGTs.

Here we collected the paddy rice soil before and during the flooding of the selected paddy soil plot and investigated the isoprenoidal (iGDGTs) and branched GDGTs (bGDGTs) distribution to estimate the flooding impact on these lipid compounds. Both the core (CL) and intact polar lipids (IPL) before and during the flooding of the paddy soil were analyzed. IPL linked to the phosphate head group are thought to lose their polar head groups quickly after cell death, leaving behind the core lipid (White et al., 1979; Harvey et al., 1986; Logemann et al., 2011). Therefore, the GDGTs linked to phosphate head group could reflect the contribution from living microorganisms or those which died very recently. Our work on paddy rice soil will help to better understand the behavior of the as-yet unknown microorganisms producing bGDGTs by assessing the parameters such as MBT, CBT, and BIT, and to further explore the potential factors controlling these proxies in this important wetland.

2 Materials and methods

2.1 Sampling

An experimental rice field at the Huazhong Agricultural University, Wuhan, in central China (30°31′29.9″N, 114°24′21.4″E) with an area of 3 m by 3 m was selected for sampling. Top bulk soil samples at the depth of 0–5 cm were collected in 2011. Five samples were collected during the dry soil period (January and February), three soil samples at the beginning of the soil flooding period (April) and five soil samples were taken one month after (in May) from the flooded soil. Soil temperature was measured in situ for each sample using a digital soil thermometer.

2.2 Soil pH determination

Samples were freeze dried and homogenized using a mortar and pestle. The soil sample was mixed with ultrapure water in a ratio of 1:2.5 (g/mL). The mixture was stirred and allowed to sit for at least 30 min. The pH values of the supernatant were measured (3×) by using a pH meter with a precision of ±0.01.

2.3 Lipid extraction and GDGTs separation

Freeze dried samples were ultrasonically extracted (3×15 min) with a solvent mixture of MeOH/DCM/phosphate buffer (2:1:0.8, v/v/v) using a modified Bligh and Dyer technique (Bligh and Dyer, 1959; Sturt et al., 2004). The supernatant of each extraction was collected and combined after the mixture was filtered. DCM and phosphate buffer were added to the combined extracts to a ratio of 1:1:0.9 (v/v/v) to achieve phase separation. DCM phase and aqueous MeOH/phosphate buffer were separated by funnel separation. The DCM phase was condensed via rotary evaporator and was dried under gentle N_2 flow. Core lipids (CL) and intact polar lipids (IPL) fractions were separated over an activated silica column (Oba et al., 2006; Liu et al., 2010). The first fraction, containing core GDGTs (CL GDGTs), was eluted with 10 mL ethyl acetate and the second, containing intact polar GDGTs (IPL GDGTs), with 10 mL methanol. Fractions were evaporated to dryness under N_2 flow. In order to cleave off the glucose and phosphate head group, acid hydrolysis was done (Pitcher et al., 2009). To this end, IPL fraction was refluxed for at least 2 h in 1.5 N HCl in MeOH. The sample was cooled down and neutralized to a pH of 5. To recover the sample, a small amount of organic-free bidistilled pure water was added and the mixture was extracted (3×) with DCM and evaporated, after collection, to dryness. In order to identify the head group type of the archaeal and bacterial GDGTs, some aliquots of the polar fraction were divided in two parts. One part was subjected to acid hydrolysis and the other to alkaline hydrolysis. Therefore, samples were refluxed for at least 2 h in KOH (1 N) in MeOH: H_2O (95/5, v/v) mixtures to cleave only the phosphate head group. After cooling down, it was neutralized to a pH of 5 and recovered as was done for acid hydrolysis. Fractions were redissolved in hexane/isopropanol (99:1, v/v) and filtered through a 0.45 μm PTFE filter prior to analysis. A known amount of C_{46} internal standard (Huguet et al., 2006) was added to quantify the GDGTs.

2.4 GDGTs Analysis

Analysis was performed using an Agilent 1200 series liquid chromatograph and triple quadrupole mass spectrometer (LC-MS/MS), equipped with an autosampler and chemstation manager software, similar to Hopmans et al. (2000) with some modifications. Samples (15 μL) were injected and separation was achieved with an Alltech Prevail Cyano Column (150 mm × 2.1 mm, 3 μm). The elution gradient follows Schouten et al. (2007) with some modifications. GDGTs were first eluted isocratically for the first 5 min with 90% A and 10% B, where A = hexane and B = hexane/isopropanol (9:1, v/v). The following linear gradient was then used: 90/10 A/B to 82/18 A/B from 5 to 45 min, followed by 100% B (10 min) to wash the column, and then 90/10 A/B to equilibrate the column. Throughout, a constant flow rate of 0.2 mL/min was used. GDGTs were ionized in an atmospheric pressure chemical ionization (APCI) source, with single ion monitoring (SIM). Quantification was achieved by comparing the peak area of $[M + 1]^+$ ions in the extracted ion chromatogram with that for the C_{46} GDGT. Samples were analyzed in duplicate and data are presented in duplicate means. Because CL and IPL fractions may not result in a full separation over silica

gel, small aliquots of the IPL fraction were analyzed using HPLC/APCI/MS without any hydrolysis to determine the amount of CL GDGTs leaked into the IPL fractions. Results showed that the pool of leaked CL into the IPL fraction is in a range of 2% of all the GDGTs measured in the CL fraction eluted with the ethyl acetate. The amount of the CL leaked into the IPL fraction was thus minor, and the correction was not done. However, the amount of CL eluted in the IPL fractions accounted for ca. 10% of all GDGTs measured in the hydrolyzed fraction in samples. Since the concentration of GDGTs in IPL fraction was low, the correction was done for these samples. Thus, the amounts of individual bGDGTs of the leaked CL into the IPL fraction were subtracted from the amounts of the corresponding GDGTs in the hydrolyzed fraction. Since the GDGTs concentration was quite low in the IPL fraction of the BK-1, BK-2 and BK-3 samples, GDGT proxies (MBT, CBT, and BIT) based on IPL GDGTs were not reported for these samples.

2.5 MBT and CBT indices

The MBT and CBT indices were calculated according to Weijers et al. (2007b):

$$\mathrm{MBT} = (\mathrm{Ia} + \mathrm{Ib} + \mathrm{Ic}) / \sum \mathrm{bGDGT}, \quad (1)$$

$$\mathrm{CBT} = -\log[(\mathrm{Ib} + \mathrm{IIb})/(\mathrm{Ia} + \mathrm{IIa})]. \quad (2)$$

The mean annual air temperature (MAT) and soil pH values were calculated using the following equations of Weijers et al. (2007b):

$$\mathrm{MAT} = (\mathrm{MBT} - 0.122 - 0.187 \times \mathrm{CBT})/0.02, \quad (3)$$

$$\mathrm{pH} = (3.33 - \mathrm{CBT})/0.38. \quad (4)$$

Revised calibration of the proxy MBT' by Peterse et al. (2012) is shown below.

$$\mathrm{MBT}' = (\mathrm{Ia} + \mathrm{Ib} + \mathrm{Ic})/(\mathrm{Ia} + \mathrm{Ib} + \mathrm{Ic} + \mathrm{IIa} + \mathrm{IIb} + \mathrm{IIc} + \mathrm{IIIa}), \quad (5)$$

$$\mathrm{MAT}' = 0.81 - 5.67 \times \mathrm{CBT} + 31.0 \times \mathrm{MBT}', \quad (6)$$

$$\mathrm{pH}' = 7.90 - 1.97 \times \mathrm{CBT}. \quad (7)$$

The BIT index was calculated according to Hopmans et al. (2004):

$$\mathrm{BIT} = (\mathrm{Ia} + \mathrm{IIa} + \mathrm{IIIa})/(\mathrm{Ia} + \mathrm{IIa} + \mathrm{IIIa} + \mathrm{crenarchaeol}). \quad (8)$$

Based on duplicate measurements of the whole data series, the average standard deviation (analytical reproducibility) was < 0.02 for the MBT, MBT′, CBT, and BIT. The uncertainties are indicated by error bars in the respective diagrams. The roman numbers in the equations above represent the corresponding GDGTs with the structures shown in Fig. 1.

3 Results and discussion

3.1 Bacterial and archaeal GDGTs head groups

In the base-hydrolyzed fractions, bGDGTs range between 93% and 94% in abundance relative to total GDGTs (Fig. 2). The ratio of IPL bGDGTs collected from the acid hydrolysis to IPLp bGDGTs obtained from base hydrolysis varies between 1 and 1.2, suggesting bGDGTs are mainly linked to the phosphoester head group. In fact, Peterse et al. (2011) detected a large part of IPL bGDGTs with phospho-hexose head group in a peat bog, and when subjected to base hydrolysis, a substantial amount of CL is yielded, which also suggests that the largest part of the IPL bGDGTs has a phospho-linked head group. In the fractions submitted to acid hydrolysis, the abundance of the isoprenoidal GDGTs (iGDGTs) ranges between 35% and 52% of the total GDGTs. This means that the archaeal GDGTs are relatively abundant in the acid fractions comparing to the alkaline fraction. In addition, the ratio of iGDGTs derived from the alkaline fraction (IPLp) to iGDGTs collected after the acid hydrolysis (IPL) varies between 0.05 and 0.3, which means that iGDGTs are mainly linked to the phosphate and/or glucose head group in our studied paddy soil. Indeed, Liu et al. (2010) found that bGDGTs linked to hexoses head group in peatlands are 5–10 times less abundant than their intact isoprenoid counterparts derived from archaea, further supporting our observation in the paddy rice field.

3.2 Isoprenoid GDGTs distribution

In dry paddy soil (non-flooded soil) and in the beginning of soil flooding, the CL GDGT-IV dominates (46% to 38%) over the other iGDGTs, with the concentration ranging from 0.61 to 5.23 $\mathrm{ng \cdot g^{-1}}$ dry weight soil (dws). However, in the samples collected from the flooded soil, the CL GDGT-V was the most dominant (42% to 53%), with a concentration ranging from 0.62 to 4.89 $\mathrm{ng \cdot g^{-1}}$ dws.

In most of the paddy soil samples analyzed, the ratio of IPL GDGT-V to their CL counterpart ranges from 0.2 to 0.6 (Fig. 3(a)). As mentioned above, IPL iGDGTs are mainly linked to glucosidic head group via ether bond, and stable during degradation (Harvey et al., 1986; Logemann et al., 2011). The CL iGDGTs occur in low abundance in our samples. Indeed, the CL can be bounded or trapped in soil matrix through organo-metallic complexes via a variety of mechanisms (Huguet et al., 2010b) and therefore, cannot be extracted by the Bligh/Dyer method used.

In addition, the ratio of IPL GDGT-V to CL GDGT-V

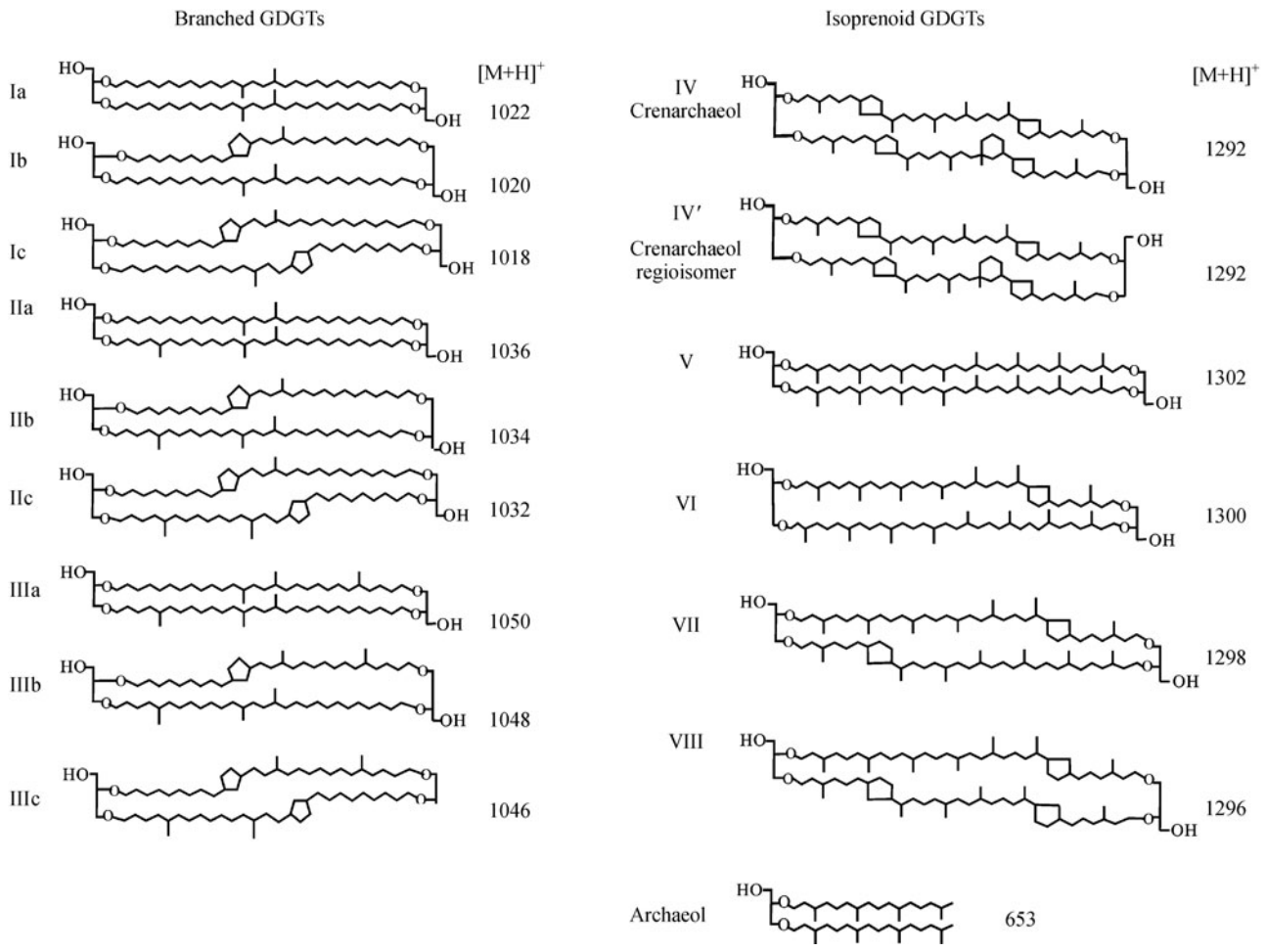

Fig. 1 Structures of the glycerol dialkyl glycerol tetraethers (GDGTs) and isoprenoid DGD analyzed in this study with corresponding $[M + H]^+$ ions and nomenclature.

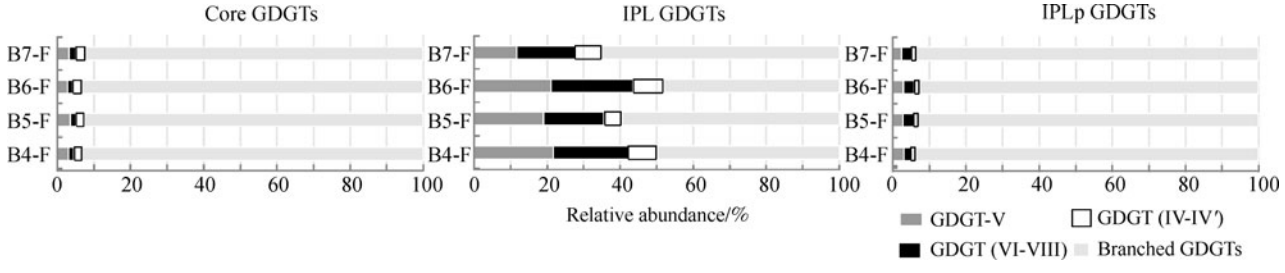

Fig. 2 Relative abundance of the isoprenoidal and branched GDGTs in the core fraction (CL GDGTs), in the acid fraction hydrolyzed (IPL GDGTs) and in the fraction submitted to the alkaline hydrolysis (IPLp GDGTs).

and of IPL crenarchaeol to CL crenarchaeol followed the same trend before and at the beginning of the soil flooding. However, the ratio of IPL crenarchaeol to CL crenarchaeol became relatively stable and had a trend different from that of GDGT-V in the flooded soil (Fig. 3(a)). This reflects that GDGT-V was mainly produced by microorganisms growing during the flooding period in the paddy soil. Thus, the IPL GDGT-V in the samples collected in the flooded soil did not reflect a refractory fraction but record the living biomass. The crenarchaeol regio-isomer shows a slight increase in abundance, a similar trend to GDGT-V, but is different from crenarchaeol in the flooded soil (data not shown). Indeed, Kim et al. (2010) noted that the regio-isomer in marine surface sediments shows a behavior different form crenarchaeol.

In the IPL fraction, the ratios of archaeol to crenarchaeol and of GDGT-V to crenarchaeol increase by 3 and 6 times in the flooded soil (Figs. 3(b) and 3(c)) than at the

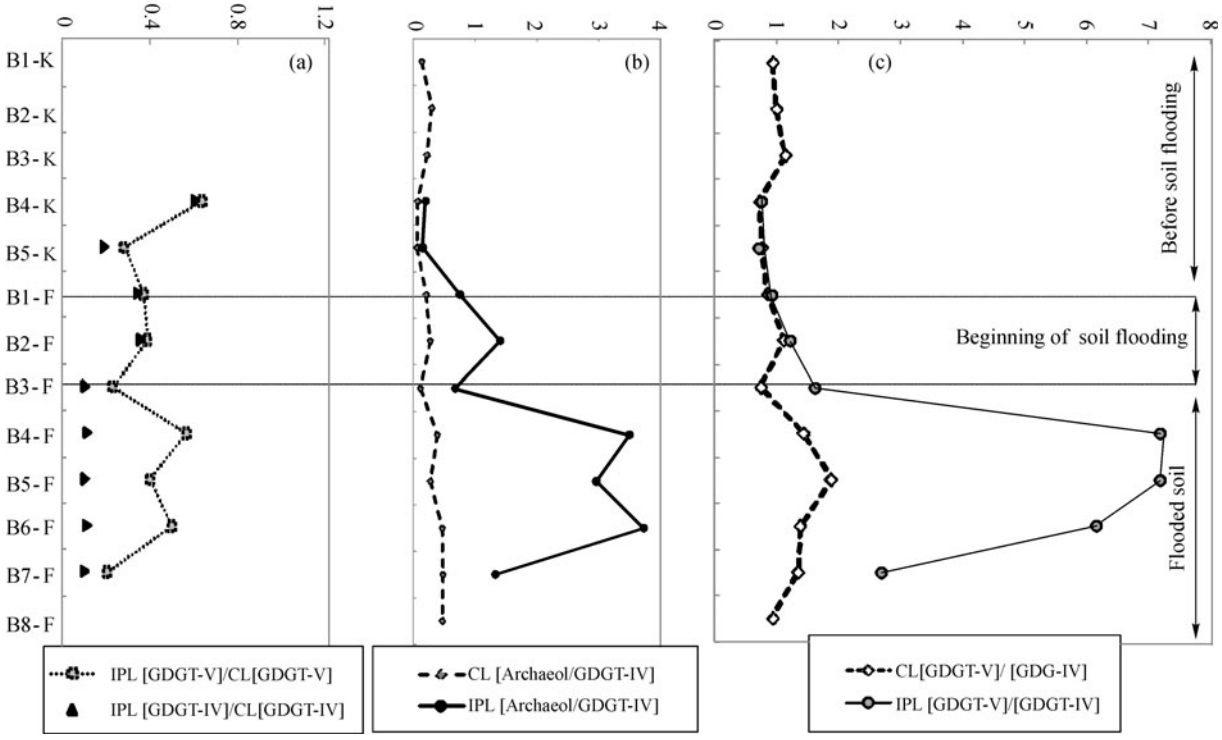

Fig. 3 Ratio profiles of (a) IPL GDGT-V and IPL GDGT-IV to their respective CL counterparts , (b) core archaeol to CL GDGT-IV and intact polar archaeol to IPL GDGT-IV , and (c) CL GDGT-V to CL GDGT-IV and IPL GDGT-V to IPL GDGT-IV.

beginning of the flooding and in dry soil, respectively. In the CL fraction, these ratios also increase but less significantly than in IPL fractions. Schouten et al. (2002) noted that the ratio of GDGT-V to crenarchaeol is dependent on temperature and varies between 0.2 and 2 in Group I thaumarchaeota. Thus, if the GDGT-V/crenarchaeol ratio is >2 in the IPL fraction, a methanogenic archaea origin may be evident for GDGT-V. Indeed, caldarchaeol (GDGT-V) can be produced by both methanogenic archaea (Koga et al., 1998a, 1998b) and thaumarchaeota (Sinninghe Damsté et al., 2002). In addition, archaeol is typically found in methanogenic euryarchaeota (Kates et al., 1993) and is known not to be produced by thaumarchaeota. The phylogenetic analyses of archaeal diversity in rhizospheres as well as in bulk soils of paddy rice fields (Großkopf et al., 1998; Liesack et al., 2000) revealed that methanogenesis in the flooded paddy rice is operated by different methanogenic groups. Therefore, an increase in GDGT-V/crenarchaeol ratio and archaeol to crenarchaeol ratio in the IPL fraction might reflect the growth of methanogenic archaea in the anoxic flooded paddy soil.

3.3 Branched GDGTs distribution

Branched GDGTs are present in all samples. GDGT-Ia is the dominant (58% to 47%) over all bGDGTs with the concentration ranging from 5.93 to 77.66 $ng \cdot g^{-1}$ dws and from 0.03 to 3.32 $ng \cdot g^{-1}$ dws in CL and IPL fractions, respectively. GDGT-IIa is the second most abundant (24% to 31%), followed by GDGT-Ib. The IPL GDGT-Ia decreases in abundance at the beginning of the soil flooding but increases later in the flooded soil. In contrast, IPL GDGT-IIa follows the opposite trend of IPL GDGT-Ia during the flooding. The other fractional bGDGTs appear to be relatively constant in abundance, and do not show any preferential trend before or during the flooding. In addition, the linear correlations between the GDGT-IIa to GDGT-Ia ratio and the MBT proxy were significant, with the coefficient being 0.95 and 0.98 for IPL and CL fraction, respectively. Since GDGT-Ia and IIa are included in the MBT and CBT calculation (Eqs. (1), (2) and (5)), we used the ratio of GDGT-IIa to GDGT-Ia to represent the patterns in the fractional abundances of bGDGTs, and to examine the general relationship between bGDGTs distribution and environmental variables.

In the CL fraction, the MBT ratio (Table 1) decreases in the flooding period (0.64 at the beginning of the soil flooding, and 0.64 to 0.60 later in the flooded soil) comparing to the dry soil (0.67–0.69). The decrease of the MBT value is due to the increase of CL GDGT-IIa in abundance in the flooded paddy soil comparing to the dry soil. Indeed, the ratio of GDGT-IIa to GDGT-Ia in the CL fraction is between 0.42 and 0.46 in the dry soil, is relatively stable at the beginning of the soil flooding (0.47), and is from 0.53 to 0.63 in the samples collected later in the flooded soil (Table 1). Our dataset (Figs. 4(a) and 4(b)) showed that the MBT proxy followed exactly the opposite trend of the GDGT-IIa to GDGT-Ia ratio for the CL and IPL fractions.

Table 1 Measured pH and temperature values, relative distribution data (bGDGT-IIa/ bGDGT-Ia), proxy values (MBT, CBT and BIT) and estimated pH and temperatures (after Weijers et al. (2007b)).

Sample type	Sample name	Soil Temp. /°C	Soil pH	IPL /CL	bGDGT (IIa/Ia)	MBT	CBT	MBT/CBT MAT/°C	CBT pH	BIT	∑bGDGT /ng·g^{-1} dws	∑ iGDGT /ng·g^{-1} dws
Dry soil	B1-K	4	5.4	CL	0.44	0.67	0.78	20.4	6.6	0.90	14.55	3.29
				IPL	n.d.	n.d.	n.d.	n.d.	n.d.	n.d.	0.28	0.44
Dry soil	B2-K	4.4	5.9	CL	0.43	0.68	0.72	21.3	6.8	0.95	16.68	1.59
				IPL	n.d.	n.d.	n.d.	n.d.	n.d.	n.d.	0.067	0.12
Dry soil	B3-K	4.1	6.2	CL	0.43	0.69	0.77	21.3	6.7	0.95	55.30	4.80
				IPL	n.d.	n.d.	n.d.	n.d.	n.d.	n.d.	0.067	0.045
Dry soil	B4-K	17.35	5.8	CL	0.45	0.67	0.79	20.0	6.6	0.9	10.52	2.09
				IPL	0.40	0.69	0.74	21.4	6.7	0,63	1.22	1.88
Dry soil	B5-K	17.7	6.4	CL	0.42	0.69	0.80	21.2	6.6	0.96	46.68	3.52
				IPL	0.42	0.67	0.74	20.6	6.7	0.77	1.24	1.12
Bg F soil	B1-F	25.3	6.6	CL	0.47	0.67	0.73	20.6	6.8	0.95	110.17	9.61
				IPL	0.58	0.61	0.72	17.8	6.8	0.63	3.05	4.58
Bg F soil	B2-F	23.8	6.9	CL	0.47	0.67	0.72	20.7	6.8	0.96	118.50	10.28
				IPL	0.59	0.61	0.72	17.9	6.8	0.66	3.51	4.92
Bg F soil	B3-F	24.5	7.5	CL	0.47	0.67	0.78	20.1	6.6	0.94	104.59	11.27
				IPL	0.52	0.63	0.74	18.8	6.8	0.84	3.55	2.81
F soil	B4-F	27.1	7.56	CL	0.53	0.64	0.76	19.1	6.7	0.97	144.68	10.89
				IPL	0.51	0.64	0.72	19.4	6.8	0.93	6.30	6.34
F soil	B5-F	27.2	n.d.	CL	0.55	0.63	0.79	18.2	6.6	0.97	115.86	9.23
				IPL	0.49	0.66	0.82	19.4	6.6	0.95	5.68	3.88
F soil	B6-F	28.2	7.6	CL	0.53	0.64	0.76	19.1	6.7	0.97	141.25	10.08
				IPL	0.51	0.65	0.74	19.6	6.8	0.92	5.01	5.37
F soil	B7-F	26.8	7.52	CL	0.60	0.61	0.75	17.6	6.7	0.96	67.42	5.68
				IPL	0.52	0.62	0.73	19.4	6.8	0.92	2.70	1.44
F soil	B8-F	27.2	7.73	CL	0.63	0.60	0.71	17.3	6.8	0.95	18.45	1.79

Note: Sample types with the letters Bg F (collected in the beginning of the soil flooding) and with the letter F (sampled later during the soil flooding); n.d. = not determined.

The IPL GDGT-IIa to IPL GDGT-Ia ratio was higher in the soil under flood than in dry soil (Fig. 5(a)). The increase of the soil temperature therefore may not be a limiting factor to the abundance of the methylated tetraether GDGT-IIa in the membrane of the living bacteria producing bGDGTs when compared to GDGT-Ia. The CL GDGT-IIa to the CL GDGT-Ia ratio was positively correlated with the temperature in the flooded soil (Fig. 5(a)). This can be due to the relatively high fractional abundance of IPL GDGT-IIa at the beginning of the soil flooding, which decreases later and may undergo a turnover, leaving behind their counterpart CL. As explained earlier, the IPL bGDGTs are mainly linked to phosphate head group, inferring a rapid turnover. However, the increase of CL GDGT-IIa/GDGT-Ia ratio in the flooded soil express a decrease of the MBT values, which is negatively correlated (R^2= 0.67) with the measured soil temperature in situ. This could explain the inconsistence between our results and the data of Weijers et al. (2007b), who found a positive correlation between the MBT values and the MAT values.

It is also noteworthy that the ratio of IPL GDGT-IIa to IPL GDGT-Ia and the measured soil pH were negatively correlated (R^2= 0.94, P = 0.0002) in the paddy flooded soil (Figs. 5(b) and 5(c)). These bacteria are thought to belong to acidobacteria phylum (Weijers et al., 2009; Sinninghe Damsté et al., 2011), which have the pH as an effective habitat filter (Jones et al., 2009). Although the GDGT-IIa/ GDGT-Ia ratio in the IPL fraction follows the opposite trend of the measured soil pH during the flooding, we cannot fully conclude that the change in the distribution of bGDGTs is under the direct control of the soil pH. Indeed, the pH increase in most acid soils is due to the reduction of Fe (III) to Fe (II) during flooding (Ponnamperuma, 1985). This change from oxic to anoxic conditions could be further proven, as explained earlier, by the increase of

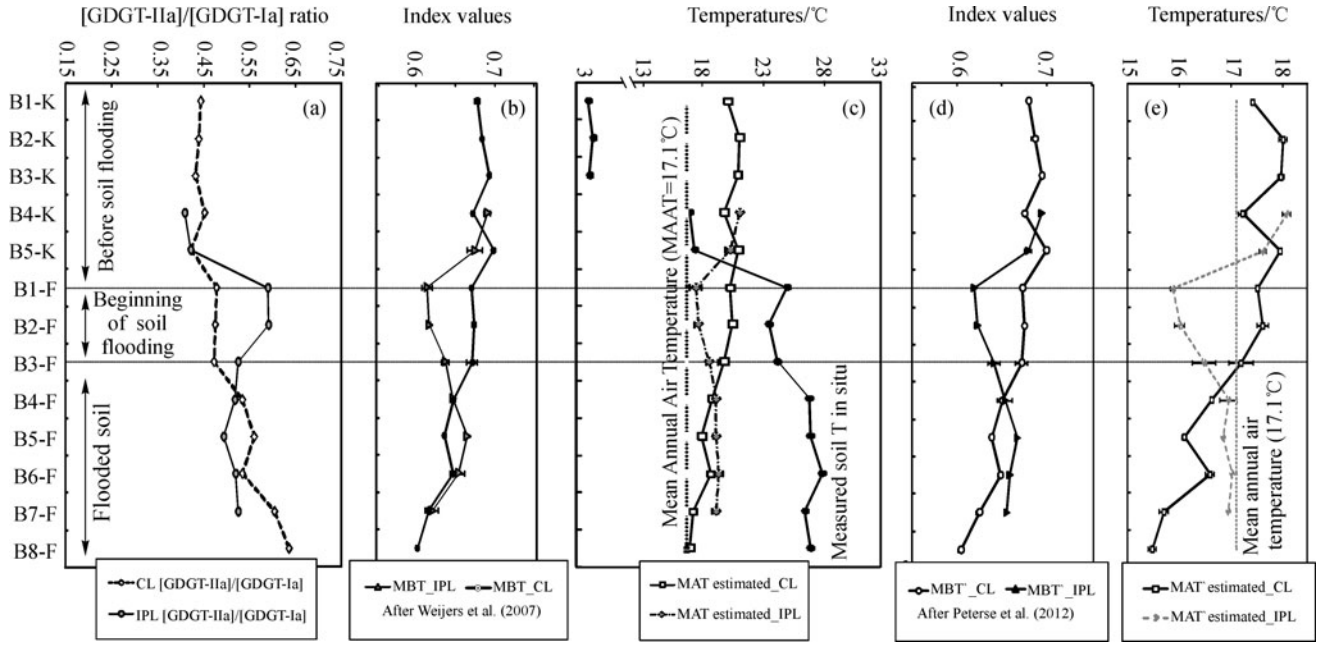

Fig. 4 CL GDGT-IIa to CL GDGT-Ia and IPL GDGT-IIa to IPL GDGT-Ia ratio profiles (a), variation in MBT (Weijers et al., 2007b) for CL and IPL fractions (b), the comparison of estimated temperatures (MAT) based on CL (open square) and IPL (grey filled diamonds), the mean annual air temperature of Wuhan (dashed line), and the measured soil temperature in situ (black circles) (c), variation in MBT` (Peterse et al., 2012) for CL and IPL fractions (d), and comparison of estimated temperatures (MAT`) based on CL (open square) and IPL (grey filled diamonds) (e).

archaeol to crenarchaeol ratio. As mentioned above, archaeol may be produced by methanogens, which are strictly anaerobic microorganisms. However, thaumarchaeota might prefer the aerobic micro-habitat when growing chemolithoautotrophically by aerobically oxidizing ammonia to nitrite (Könneke et al., 2005). Indeed, Sinninghe Damsté et al. (2012) cultured Group I.1a and I.1b Thaumarchaeota and measured their growth through their consumption of ammonium under aerobic inoculation. Thus, we speculate that the bGDGTs distribution change may be due to the variation of the redox conditions, which is in turn affected by the soil flooding. This would suggest an aquatic influence on the distribution of the bGDGTs in soils. In addition, the measured pH values and the ratio of GDGT-IIa to GDGT-Ia in the CL fraction were positively correlated. This is consistent with the result of Weijers et al. (2007b), who found a negative correlation between the CL MBT and the soil pH values.

To examine whether the estimated temperature (Weijers et al., 2007b) is reliable in our study, we calculated the MAT' following the calibration dataset of Peterse et al. (2012). The temperature estimates based on both IPL and CL bGDGTs are lower in the flooded soil than in the dry soil (Figs. 4(c) and 4(e)). However, the temperatures (MAT) calculated using the original global soil calibration (Weijers et al., 2007b) are greater than the reconstructed temperatures (MAT′) by the new calibration (Peterse et al., 2012), by an average of 2.8°C for the CL fraction and 2.5°C for the IPL fraction, but the variation trends of the temperature reconstructed remain unchanged. The two calibrations produce the declined temperature in the flooded soil.

It is somewhat surprising that there is no obvious relationship between the measured soil pH values and the CBT-derived pH (Figs. 5(d), 5(e) and 5(f)). However, we observed that the CBT proxy has good prediction when the average pH value was calculated for all soil samples, regardless of the soil water content. Indeed, while the average of the measured pH values is 6.7 (±0.7), the CBT-derived pH (Weijers et al., 2007b) average is 6.7 (±0.07) and 6.7 (±0.1), respectively, based on CL and IPL. In addition, the CBT-derived pH` (Peterse et al., 2012) average is 6.39 (±0.06) and 6.42 (±0.05), respectively, for CL and IPL. Most of the cyclic GDGT compounds identified as driving the relationship with pH (e.g., GDGT-Ib, GDGT-IIb; Weijers et al., 2007b) does not show any preferential trend between the flooded and non-flooded paddy soil. This may explain the reconstructed soil pH is independent of the measured soil pH trend.

Our dataset showed that there are variations in the MBT-derived temperature between the dry and the flooded soil, but no clear trend is observed in the CBT-derived soil pH. Our results also showed that the bGDGTs are mainly linked to the phosphate head group, which means that the IPL bGDGT reflects the living bacteria. Thus, at the beginning of and during the flooding, the living bacterial

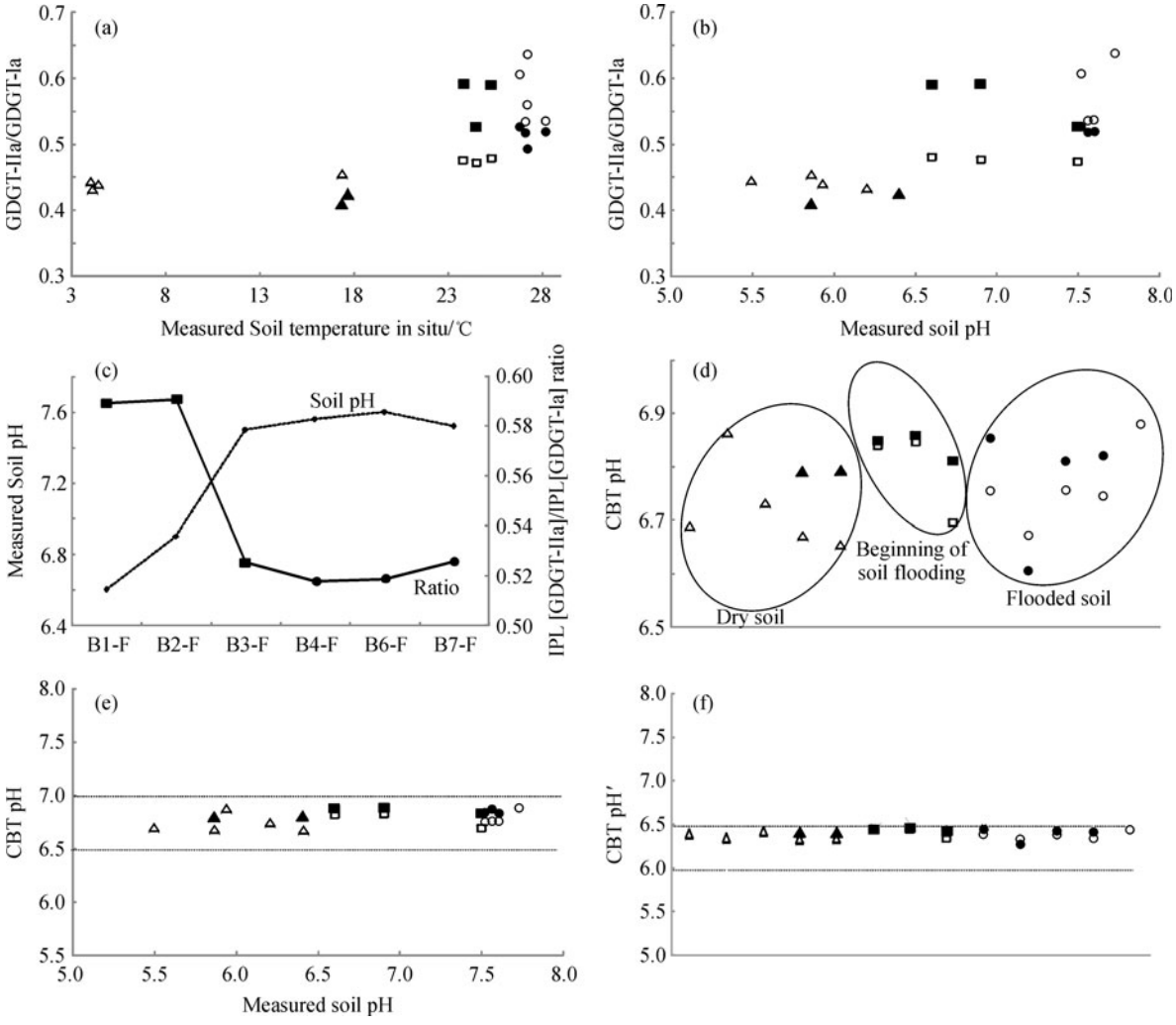

Fig. 5 Cross-plots between IPL GDGT-IIa to IPL GDGT-Ia ratio and measured soil temperature (a), correlation between IPL GDGT-IIa to IPL GDGT-Ia ratio and soil pH (b), IPL GDGT-IIa to IPL GDGT-Ia ratio and soil pH in the beginning of soil flooding and during the flooding (c), CBT pH (Weijers et al., 2007b) (d), measured soil pH vs. CBT derived pH (e), and CBT pH′ (Peterse et al., 2012) (f). Dry soil (triangles), beginning of the soil flooding (squares) and during the soil flooding (circles). IPL fractions (black triangles, squares and circles) and CL fractions (open triangles, squares and circles).

community (or communities) synthesizing bGDGTs may change its (or their) cell membrane GDGT distributions only by varying the amount of methyl groups on their carbon chains to adapt to the soil flooding conditions.

Tierney and Russell (2009) and Tierney et al. (2010, 2012) found that bGDGTs in surface lake sediments had CBT values different from, and MBT values lower than, soils from the lake catchments. Indeed, they found that more methylated bGDGTs were produced in the lacustrine sediment than in the soil, indicating a different bacterial community synthesizing GDGTs in the aquatic environment.

However, from our data it is difficult to fully conclude that the bGDGTs distribution change is due to the change of the bacterial community producing bGDGTs or just a variation of the membrane GDGTs distribution of the same bacterial communities, which are thriving in the dry as well as in the flooded soil, due to the redox condition change resulting from flooding. Nonetheless, the bGDGT distributions are demonstrated here to change with the flooded conditions within the paddy rice soil selected.

3.4 BIT index

The BIT index is based on the relative abundance of bGDGTs versus crenarchaeol (Hopmans et al., 2004). Our results (Table 1) showed a slight increase in BIT index, which varies between 0.90 and 0.96, in the dry paddy soil, and from 0.94 to 0.97 during the flooding for CL fraction. In the IPL fraction, however, the BIT index is 0.63 and 0.77 in the dry soil and sharply increases to 0.95 in the flooded soil.

As explained earlier, the IPL GDGT-V to the IPL GDGT-IV ratio is relatively high in the flooded soil studied. This is due to the increase in the relative abundance of caldarchaeol (GDGT-V), which may be produced by anaerobic methanogens (Koga et al., 1998a, b; Pancost et al., 2001). However, IPL crenarchaeol (GDGT-IV) was relatively stable in abundance in the flooded soil. In a similar way, the increase of the BIT index in the flooded soil, in both CL and IPL fractions, could be attributed to the increase in the total abundance of major bGDGTs (Ia, IIa and IIIa). As explained earlier, the IPL bGDGTs are mainly bounded to phosphoester head group, which might reflect the existence of living bacteria producing bGDGTs in the flooded soil. This may support the idea of the preference of the bGDGT-producing bacteria for the anoxic habitats and the relatively higher production of bGDGTs in the flooded paddy soil. Indeed, during the flooding, the paddy soil becomes anoxic and the oxygen never penetrates downward more than 3–6 mm from the floodwater- soil boundary layer (Liesack et al., 2000). Therefore, the environment becomes favorable for the activity of diverse anaerobic microorganisms such as methanogens and the bacteria producing bGDGTs. In fact, these bacteria are considered as facultative anaerobic (Weijers et al., 2006; Huguet et al., 2010a). In addition, the pH of about 7 favors microbial activity because the main microorganisms in reduced soils are anaerobic, which function best at a pH of about 7 (Ponnamperuma, 1985). Thus, the methane (CH_4) formation is favored by the pH change in the submerged soils (Ponnamperuma, 1985). However, as mentioned earlier, the ammonia oxidizing archaea (AOA), the predominant source of crenarchaeol (Pitcher et al., 2011), may have a higher affinity to oxygen or carbon dioxide, which may explain their predominance in the rhizosphere of the rice plant over that in the bulk of the flooded paddy soil (Chen et al., 2008). Considering that the bacteria producing bGDGTs and thaumarchaeota might proliferate in different conditions of aeration, the BIT index could be used to indicate the degree of aeration in soil and paleosol.

In addition, the ratio of GDGT-V to crenarchaeol is correlated positively with the BIT index in the CL and IPL fractions (Figs. 6(a) and 6(b)). Weijers et al. (2006) found the same correlation between the sum of major bGDGTs (IIIa, IIa, and Ia) and caldarchaeol along the peat bog profile. This positive relationship between the GDGT-V and the sum of major bGDGTs (Ia, IIa, and IIIa) might lead us to speculate that methanogens and the bacteria producing bGDGTs may belong to the same microbial food-web in the paddy soil. Chin et al. (1998) noted that in the flooded paddy soil, the anaerobic degradation starts with the fermenting bacteria which excrete enzymes that hydrolyze the polysaccharides and convert the resulting sugar monomers to H_2, alcohols, and fatty acids, which after further degradation could finally serve as substrates for methanogens. This is further supported by Pancost and

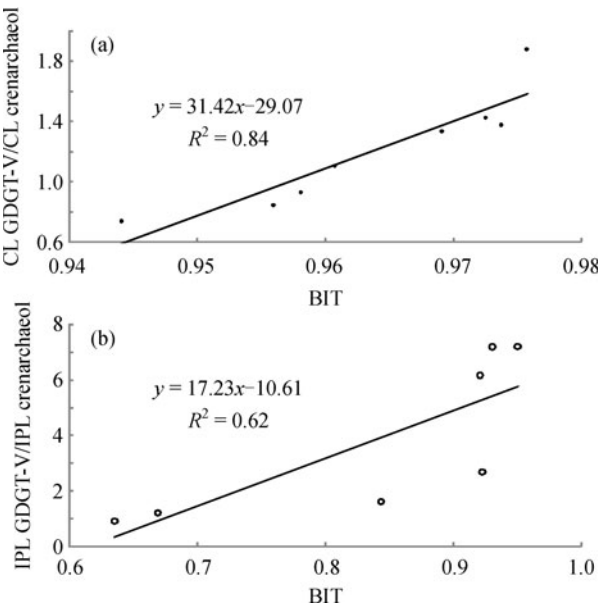

Fig. 6 Correlation of BIT index with the GDGT-V to crenarchaeol ratio for CL fraction (a) and IPL fraction (b).

Sinninghe Damsté. (2003) and Weijers et al. (2010), who suggested that the bacteria producing bGDGTs could be involved in the fermentation of labile organic matter that potentially generates substrates for other anaerobic microorganisms such as methanogens.

4 Conclusions

Data obtained from dry and flooded paddy rice soil in Huazhong Agricultural University in central China indicated a change in the CL and IPL GDGTs distribution, which is probably the impact of the soil water content on the variation in lipid composition. The archaeol to crenarchaeol ratio and the GDGT-V to crenarchaeol ratio increase in the flooded soil for both the CL and IPL fractions, indicating a change in microbial communities and an occurrence of strictly anaerobic microorganisms (methanogens). The good correlation between the GDGT-IIa/GDGT-Ia ratio and the measured pH, which is controlled by the redox conditions, led us to speculate that the bGDGTs distribution may be affected by the redox condition, hence by the flooding. Clearly, future work should focus on the effect of the water content on the GDGTs distribution, which will help to provide more direct evidence of the impact of the redox condition on the GDGTs distribution. The BIT values are higher in the soil under flooding than in the dry soil, indicating the production of bGDGTs in the flooded soil. These bacteria producing bGDGTs may thus proliferate in anoxic habitats provided by the soil flooding. Our results are consistent with the previous findings that these bacteria are facultatively anaerobic. It is of importance to note that

the archaeol to crenarchaeol ratio, together with the BIT index, could be used to indicate the aeration condition in soil and paleosoil, as the microorganisms producing archaeol and bGDGTs may require aeration conditions different from thaumarchaeota, the microorganisms producing crenarchaeol.

Acknowledgements We would thank Dr. WeiHua Ding for analytical assistance with the HPLC-MS equipment. This work was supported by the National Basic Research Program of China (No. 2011CB808800), the National Natural Science Foundation of China (Grant Nos. 40930210 and 40921062) and the 111 program (B08030) in China.

References

Bligh E G, Dyer W J (1959). A rapid method of total lipid extraction and purification. Can J Biochem Physiol, 37(8): 911–917

Chen X P, Zhu Y G, Xia Y, Shen J P, He J Z (2008). Ammonia-oxidizing archaea: important players in paddy rhizosphere soil? Environ Microbiol, 10(8): 1978–1987

Chin K J, Rainey F A, Janssen P H, Conrad R (1998). Methanogenic degradation of polysaccharides and the characterization of polysaccharolytic clostridia from anoxic rice field soil. Syst Appl Microbiol, 21(2): 185–200

Großkopf R, Stubner S, Liesack W (1998). Novel euryarchaeotal lineages detected on rice roots and in the anoxic bulk soil of flooded rice microcosms. Appl Environ Microbiol, 64(12): 4983–4989

Harvey H R, Fallon R D, Patton J S (1986). The effect of organic matter and oxygen on the degradation of bacterial membrane lipids in marine sediments. Geochim Cosmochim Acta, 50(5): 795–804

Hopmans E C, Schouten S, Pancost R D, van der Meer M T J, Sinninghe Damsté J S (2000). Analysis of intact tetraether lipids in archaeal cell material and sediments by high performance liquid chromatography/atmospheric pressure chemical ionization mass spectrometry. Rapid Commun Mass Spectrom, 14(7): 585–589

Hopmans E C, Weijers J W H, Schefuß E, Herfort L, Sinninghe Damsté J S, Schouten S (2004). A novel proxy for terrestrial organic matter in sediments based on branched and isoprenoid tetraether lipids. Earth Planet Sci Lett, 224(1–2): 107–116

Huguet A, Fosse C, Laggoun-Défarge F, Toussaint M L, Derenne S (2010a). Occurrence and distribution of glycerol dialkyl glycerol tetraethers in a French peat bog. Org Geochem, 41(6): 559–572

Huguet A, Fosse C, Metzger P, Fritsch E, Derenne S (2010b). Occurrence and distribution of non-extractable glycerol dialkyl glycerol tetraethers in temperate and tropical podzol profiles. Org Geochem, 41(8): 833–844

Huguet A, Wiesenberg G L B, Gocke M, Fosse C, Derenne S (2012). Branched tetraether membrane lipids associated with rhizoliths in loess: Rhizomicrobial overprinting of initial biomarker record. Org Geochem, 43: 12–19

Huguet C, Hopmans E C, Febo-Ayala W, Thompson D H, Sinninghe Damsté J S, Schouten S (2006). An improved method to determine the absolute abundance of glycerol dibiphytanyl glycerol tetraether lipids. Org Geochem, 37(9): 1036–1041

Jones R T, Robeson M S, Lauber C L, Hamady M, Knight R, Fierer N (2009). A comprehensive survey of soil acidobacterial diversity using pyrosequencing and clone library analyses. ISME J, 3(4): 442–453

Kates M, Kushner D J, Matheson A T (1993). The biochemistry of Archaea (Archaebacteria). Amsterdam: Elsevier Science Publishers

Kim J H, van der Meer J, Schouten S, Helmke P, Willmott V, Sangiorgi F, Koç N, Hopmans E C, Sinninghe Damsté J S (2010). New indices and calibrations derived from the distribution of crenarchaeal isoprenoid tetraether lipids: Implications for past sea surface temperature reconstructions. Geochim Cosmochim Acta, 74(16): 4639–4654

Koga Y, Kyuragi T, Nishihara M, Sone N (1998a). Did archaeal and bacterial cells arise independently from noncellular precursors? A hypothesis stating that the advent of membrane phospholipid with enantiomeric glycerophosphate backbones caused the separation of the two lines of descent. J Mol Evol, 46(1): 54–63

Koga Y, Morii H, Akagawa-Matsushita M, Ohga M (1998b). Correlation of polar lipid composition with 16S rRNA phylogeny in methanogens. Further analysis of lipid component parts. Biosci Biotechnol Biochem, 62(2): 230–236

Könneke M, Bernhard A E, de la Torre J R, Walker C B, Waterbury J B, Stahl D A (2005). Isolation of an autotrophic ammonia-oxidizing marine archaeon. Nature, 437(7058): 543–546

Liesack W, Schnell S, Revsbech N P (2000). Microbiology of flooded rice paddies. FEMS Microbiol Rev, 24(5): 625–645

Liu X L, Leider A, Gillespie A, Gröger J, Versteegh G J M, Hinrichs K U (2010). Identification of polar lipid precursors of the ubiquitous branched GDGT orphan lipids in a peat bog in Northern Germany. Org Geochem, 41(7): 653–660

Logemann J, Graue J, Köster J, Engelen B, Rullkötter J, Cypionka H (2011). A laboratory experiment of intact polar lipid degradation in sandy sediments. J Biosci, 8: 3289–3321

Loomis S E, Russell J M, Sinninghe Damsté J S (2011). Distributions of branched GDGTs in soils and lake sediments from western Uganda: Implications for a lacustrine paleothermometer. Org Geochem, 42(7): 739–751

Lu Y, Conrad R (2005). In situ stable isotope probing of methanogenic archaea in the rice rhizosphere. Science, 309(5737): 1088–1090

Lu Y, Lueders T, Friedrich M W, Conrad R (2005). Detecting active methanogenic populations on rice roots using stable isotope probing. Environ Microbiol, 7(3): 326–336

Oba M, Sakata S, Tsunogai U (2006). Polar and neutral isopranyl glycerol ether lipids as biomarkers of archaea in near-surface sediments from the Nankai Trough. Org Geochem, 37(12): 1643–1654

Pancost R D, Hopmans E, Sinninghe Damsté J S (2001). Archaeal lipids in Mediterranean cold seeps: molecular proxies for anaerobic methane oxidation. Geochim Cosmochim Acta, 65(10): 1611–1627

Pancost R D, Sinninghe Damsté J S (2003). Carbon isotopic compositions of prokaryotic lipids as tracers of carbon cycling in diverse settings. Chem Geol, 195(1–4): 29–58

Peterse F, Prins M A, Beets C J, Troelstra S R, Zheng H, Gu Z, Schouten S, Sinninghe Damsté J S (2011). Decoupled warming and monsoon precipitation in East Asia over the last deglaciation. Earth Planet Sci Lett, 301(1–2): 256–264

Peterse F, van der Meer J, Schouten S, Weijers J W H, Fierer N, Jackson R B, Kim J H, Sinninghe Damsté J S (2012). Revised calibration of the MBT-CBT paleotemperature proxy based on branched tetraether

membrane lipids in surface soils. Geochim Cosmochim Acta, 96: 215–229

Pitcher A, Hopmans E C, Schouten S, Sinninghe Damsté J S (2009). Separation of core and intact polar archaeal tetraether lipids using silica columns: insights into living and fossil biomass contributions. Org Geochem, 40(1): 12–19

Pitcher A, Wutcher C, Siddenberg K, Schouten S, Sinninghe Damsté J S (2011). Crenarchaeol tracks winter blooms of ammonia-oxidizing Thaumarchaeota in the coastal North Sea. Limnol Oceanogr, 56(6): 2308–2318

Ponnamperuma F N (1985). Chemical kinetics of wetland rice soils relative to soil fertility. In: Proceeding of wetland soils: characterization, classification and utilization. Philippines, International Rice Research Institute, 71–89

Revsbech N, Pedersen O, Reichardt W, Briones A (1999). Microsensor analysis of oxygen and pH in the rice rhizosphere under field and laboratory conditions. Biol Fertil Soils, 29(4): 379–385

Schouten S, Hopmans E C, Schefuß E, Sinninghe Damsté J S (2002). Distributional variations in marine crenarchaeotal membrane lipids: a new tool for reconstructing ancient sea water temperatures? Earth Planet Sci Lett, 204(1–2): 265–274

Schouten S, Huguet C, Hopmans E C, Kienhuis M V M, Sinninghe Damsté J S (2007). Improved analytical methodology and constraints on analysis of the TEX86 paleothermometer by high performance liquid chromatography/atmospheric pressure chemical ionization-mass spectrometry. Anal Chem, 79(7): 2940–2944

Sinninghe Damsté J S, Schouten S, Hopmans E C, van Duin A C, Geenevasen J A (2002). Crenarchaeol the characteristic core glycerol dibiphytanyl glycerol tetraether membrane lipid of cosmopolitan pelagic crenarchaeota. J Lip Res, 43(10): 1641–1651

Sinninghe Damsté J S, Rijpstra W I C, Hopmans E C, Weijers J W H, Foesel B U, Overmann J, Dedysh S N (2011). 13,16-Dimethyl octacosanedioic acid (iso-diabolic acid), a common membrane-spanning lipid of Acidobacteria subdivisions 1 and 3. Appl Environ Microbiol, 77(12): 4147–4154

Sinninghe Damsté J S, Rijpstra W I C, Hopmans E C, Jung M Y, Kim J G, Rhee S K, Stieglmeier M, Schleper C (2012). Intact Polar and Core Glycerol Dibiphytanyl Glycerol Tetraether Lipids of Group I. 1a and I. 1b Thaumarchaeota in Soil. Appl Environ Microbiol, 78(19): 6866–6874

Sturt H F, Summons R E, Smith K, Elvert M, Hinrichs K U (2004). Intact polar membrane lipids in prokaryotes and sediments deciphered by high-performance liquid chromatography/electrospray ionization multistage mass spectrometry—new biomarkers for biogeochemistry and microbial ecology. Rapid Commun Mass Spectrom, 18(6): 617–628

Tierney J E, Russell J M (2009). Distributions of branched GDGTs in a tropical lake system: implications for lacustrine application of the MBT/CBT palaeoproxy. Org Geochem, 40(9): 1032–1036

Tierney J E, Russell J M, Eggermont H, Hopmans E C, Verschuren D, Sinninghe Damsté J S (2010). Environmental controls on branched tetraether lipid distributions in tropical East African lake sediments. Geochim Cosmochim Acta, 74(17): 4902–4918

Tierney J E, Schouten S, Pitcher A, Hopmans E C, Sinninghe Damsté J S (2012). Core and intact polar glycerol dialkyl glycerol tetraethers (GDGTs) in Sand Pond, Warwick, Rhode Island (USA): insights into the origin of lacustrine GDGTs. Geochim Cosmochim Acta, 77: 561–581

Weijers J W H, Panoto E, van Bleijswijk J, Schouten S, Rijpstra W I C, Balk M, Stams A J M, Sinninghe Damsté J S (2009). Constraints on the biological source (s) of the orphan branched tetraether membrane lipids. Geomicrobiol J, 26(6): 402–414

Weijers J W H, Schefuss E, Schouten S, Sinninghe Damsté J S (2007a). Coupled thermal and hydrological evolution of tropical Africa over the last deglaciation. Science, 315(5819): 1701–1704

Weijers J W H, Schouten S, Hopmans E C, Geenevasen J A J, David O R P, Coleman J M, Pancost R D, Sinninghe Damsté J S (2006). Membrane lipids of mesophilic anaerobic bacteria thriving in peats have typical archaeal traits. Environ Microbiol, 8(4): 648–657

Weijers J W H, Schouten S, van den Donker J C, Hopmans E C, Sinninghe Damsté J S (2007b). Environmental controls on bacterial tetraether membrane lipid distribution in soils. Geochim Cosmochim Acta, 71(3): 703–713

Weijers J W H, Wiesenberg G L B, Bol R, Hopmans E C, Pancost R D (2010). Carbon isotopic composition of branched tetraether membrane lipids in soils suggest a rapid turnover and a heterotrophic life style of their source organism (s). Biogeosciences, 7(9): 2959–2973

White D, Davis W, Nickels J, King J, Bobbie R (1979). Determination of the sedimentary microbial biomass by extractible lipid phosphate. Oecologia, 40(1): 51–62

Yang H, Ding W, Wang J, Jin C, He G, Qin Y, Xie S (2012). Soil pH impact on microbial tetraether lipids and terrestrial input index (BIT) in China. Science China (Earth Sciences), 55(2): 236–245

Yang H, Ding W, Zhang C L, Wu X, Ma X, He G, Huang J, Xie S (2011). Occurrence of tetraether lipids in stalagmites: Implications for sources and GDGT-based proxies. Org Geochem, 42(1): 108–115